Science of the Total Environment 752 (2021) 141770

Contents lists available at ScienceDirect

Science of the Total Environment

journal homepage: www.elsevier.com/locate/scitotenv

Spatiotemporal tradeoffs and synergies in vegetation vitality and poverty transition in rocky desertification area

Sen Zhao [a,b,c], Xiuqin Wu [a,b,c,*], Jinxing Zhou [a,b,c], Paulo Pereira [d]

[a] School of Soil and Water Conservation, Beijing Forestry University, Beijing 100083, China
[b] Key Laboratory of Soil and Water Conservation of State Forestry Administration, Beijing Forestry University, Beijing 100083, China
[c] Jianshui Research Station, School of Soil and Water Conservation, Beijing Forestry University, Beijing 100083, China
[d] Environment Management Laboratory, Mykolas Romeris University, Ateities g. 20, LT-08303 Vilnius, Lithuania

HIGHLIGHTS

- We assessed the space-time relation of vegetation vitality and poverty transition.
- Vegetation restoration helped poverty alleviation in poor karst counties.
- Karst vegetation was more affected by both of poverty and rocky desertification.
- Trade-offs relation in poverty and vegetation is high in the quick green area.
- Ecological assessments should consider poverty in the rocky desertification area.

GRAPHICAL ABSTRACT

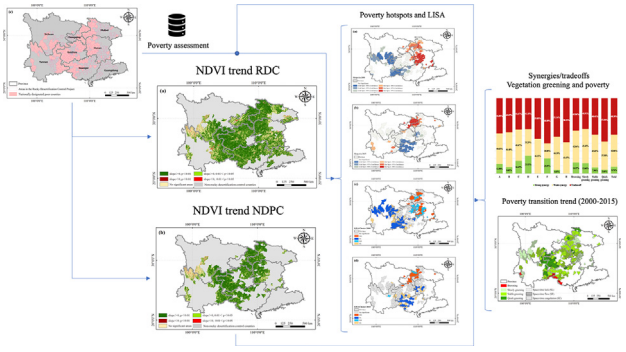

ARTICLE INFO

Article history:
Received 17 June 2020
Received in revised form 14 August 2020
Accepted 16 August 2020
Available online 19 August 2020

Editor: Fernando A.L. Pacheco

Keywords:
Karst rocky desertification
Vegetation restoration
Poverty alleviation
Spatiotemporal relationship
Drivers

ABSTRACT

Vegetation recovery and poverty alleviation are critical problems in the karst national designed poor counties (NPDC) in southwest China. However, little information is available about the relationship between poverty and vegetation dynamics in these areas. In this study, we used remote sensing and statistical datasets from 2000 to 2015 to identify the relations between vegetation dynamics and poverty among the NPDC in southwest rocky desertification areas. We estimated the vegetation dynamics using the Normalized Difference Vegetation Index and poverty with the rural per capita net income. Local indicator of spatial association and the space-time transition type of poverty were applied to identify spatial patterns of the poverty spatial distribution relationship and transition. Also, poverty, natural and ecological governance factors were assessed using the Geodetector method to uncover the driving factors of karst vegetation. The results showed that vegetation increased significantly ($p < 0.05$) in karst NPDC (82.82%) and rocky desertification control counties (78.77%). The karst NPDC was significantly clustered. The hot spots of rural per capita net income changed from west and north (2000) to only north (2015) and cold spots changed from east and south (2000) to only south (2015). The rural per capita net income spatiotemporal transition was higher in 2000 than in 2015. We found a weak synergy between vegetation change and poverty type transition in 42.86% of the browning counties, 45.45% in the slowly greening counties, and 43.65% in stable greening counties. However, 57.50% of counties in the quick greening counties showed a tradeoff relationship with the poverty type transition. The rocky desertification rate and ecological engineering measures affected vegetation dynamics importantly. The results will help decision-makers to understand the interdependence between vegetation and poverty. This will contribute to better policies formulation to tackle poverty in the karst rocky desertification area.

Abbreviations: NPDC, national designed poor counties; RDC, rocky desertification counties; RPI, rural per capita net income; LISA, local indicator of spatial association.

* Corresponding author at: School of Soil and Water Conservation, Beijing Forestry University, Beijing 100083, China.
E-mail addresses: zhaosen@bjfu.edu.cn (S. Zhao), wuxq@bjfu.edu.cn (X. Wu), zjx001@bjfu.edu.cn (J. Zhou), pereiraub@gmail.com (P. Pereira).

https://doi.org/10.1016/j.scitotenv.2020.141770
0048-9697/

1. Introduction

Human activities and climate change have a substantial impact on vegetation dynamics and ecosystems vitality (Defriez and Reuman, 2017; Smith et al., 2019; Song et al., 2018; Zhu et al., 2016). The complex interactions between land use and climate change will increase land degradation, especially in vulnerable ones such as karst ecosystems (Gutiérrez et al., 2014). Karst occupies more than 10% of the land surface, and it is extremely vulnerable to desertification (Ford and Williams, 2007). Rocky desertification occurs in several countries such as in Belize, Guatemala, Mexico of North America, Israel of the Middle East, and East and Southeast Asia, including the Ryukyu Islands of Japan and Indonesia (S. Zhao et al., 2020; R. Zhao et al., 2020). Due to human activities, karst desertification is also widely distributed in the European Mediterranean basin (Ezio et al., 1999; Pardo-Igúzquiza et al., 2012), in areas such as the Dinaric Karst (Gams and Gabrovec, 1999). One of the most well-known examples is located in Southwest China (Jiang et al., 2014). The region had experienced severe degradation through rocky karst desertification between the 1950s and 1990s (Zhang et al., 2017), increasing soil degradation (Wang et al., 2004; J.Y. Zhang et al., 2016). However, in previous years, a regreening trend was observed in this area (Chen et al., 2019). Restoration measures designed by the National Forestry and Grassland Administration were carried out in 465 counties of southwest China to mitigate rocky desertification. Two hundred seventeen of these counties were classified as nationally designated poor counties (NDPC) by the Chinese government. Due to these restrictions, and the unique geological conditions, the development in these NDPC was limited, resulting in high poverty levels (Desmond, 2017; Pang et al., 2018).

Because of the limited resources in the karst rocky desertification area, life is harsh. Therefore, the interaction between poverty and the environment needs to be assessed and is critical to supporting sustainable development measures (Moser, 1998; Tallis et al., 2008; Tallis and Kareiva, 2006). Here, poverty is a consequence of the harsh environment and land degradation (Jiang et al., 2014). The per-capita income is low compared to neighbor regions (Ravallion and Chen, 2019). In recent years, several measures were carried out with success for vegetation restoration (e.g., grain for green) and poverty alleviation. Since 1998 several projects were carried out in Southwest China to reduce land degradation. Although the effect of governance on vegetation restoration has been studied, its impact on poverty and its relation between poverty and vegetation restoration received little attention. Therefore, the assessment of this relationship is meaningful for decision-makers to incorporate into plans for this area.

Vegetation recovery plays an essential role in ecological restoration and has implications in the socio-economic status of the environment (Zhu et al., 2016). For example, the environmental Kuznets Curve expresses the relation between the environment and economy factors (Dinda, 2004), and allows to identify the relation between vegetation and poverty. In recent years, poverty decreased in the Chinese karst area due to vegetation restoration (Wang et al., 2004; Chen et al., 2019; Montalvo and Ravallion, 2010). However, macro socio-economic circumstances do not encourage local farmers to protect the environment in karst rocky desertification in southwest China (Yan and Cai, 2015). This means that vegetation recovery and poverty alleviation have different trends. However, sustainable land use management can balance human demand and environment quality in rocky desertification in a karst area (Zhang et al., 2020). Nevertheless, the relation between vegetation restoration and poverty alleviation in this area is not entirely understood. Therefore, it is vital to identify the relations between vegetation restoration and poverty reduction. It is vital to identify if this relation is synchronized or delayed, and what are the driving factors that influence this relationship in space and time. (Desmond, 2017; Zhou and Liu, 2019).

Normalized difference vegetation index (NDVI) is a widely used method to detect vegetation greening and suitable to assess restoration impacts (Liu et al., 2015; Pettorelli et al., 2005). The maximization synthesis method used in NDVI spatial analysis has been applied to measure the maximum vegetation per unit. However, the relation between NDVI and restoration practices in the karst area is variable and in space, and the effects are lagged. (Cheng et al., 2017; Tong et al., 2018; J.Y. Zhang et al., 2016). The impacts of restoration depend on several environmental and socio-economical aspects (e.g., topography, precipitation, management, population dynamics). Therefore, it is a highly dynamic process (Liu et al., 2018; Wu et al., 2015; Xu and Zhang, 2018). Local and global spatial autocorrelation analysis are useful methods for identifying vegetation restoration and poverty space characters (Cai et al., 2017; He et al., 2019). Local spatial autocorrelation path analysis (LISA) is used to find discrete objects' change process (Ord and Getis, 2010; Sokal et al., 1998). LISA space-time transitions can identify the clusters (space-time lock, flow, and coagulation).

Tradeoffs and synergies assessments have been widely applied in ecosystem services studies to assess human-land relationships (Bennett et al., 2009). In this work, the identification of tradeoffs and synergies analysis is essential to study the relation of vegetation restoration and poverty transition in space and time (X. Liu et al., 2019; Y. Liu et al., 2019; Schirpke et al., 2019). This can assess whether human wellbeing and restoration measures are interdependent. The Geo-detector model can identify the degree of influence of the different driving factors and evaluate the importance of each factor. This method has been used in the relations between the environment and humans to solve vague and uncertain problems (Gao and Wang, 2019; H. Wang et al., 2019; K. Wang et al., 2019), typical in social geography (Su et al., 2020; S. Zhao et al., 2020; R. Zhao et al., 2020). It can examine the stratified heterogeneity of every single factor. The causal relationship between the two factors can be detected by examining the spatial distribution of the two factors. The interaction detector can be used to evaluate whether the combination of two factors will increase or decrease the single dependent factor's explanatory power. Also, the collinearity of the dependent variable will not affect the accuracy of the method (Wang et al., 2016). In our study, the Geo-detector was applied to identify the most problematic interaction effects on the vegetation restoration degree. Poverty spatial heterogeneity was overlooked in previous studies, and very little information is available about the interdependence between vegetation restoration and poverty. Therefore, in this work, we used the poverty space transition as one factor. This will help to understand the spatiotemporal interdependence between poverty and vegetation restoration.

This paper aims to study the spatiotemporal tradeoffs and synergies in vegetation vitality and poverty transition in the rocky desertification area. The specific objectives are to: 1) detect the vegetation trend and poverty situation and assess the spatiotemporal vegetation dynamic and poverty transition dynamic, 2) evaluate the importance of poverty transition on vegetation restoration by analyzing multivariate factors relationship that rules it and 3) identify the regional tradeoffs and synergies relationship in vegetation restoration and poverty transition. This work will be extremely relevant to decision-makers to understand the relations between vegetation status and poverty and the factors that influence it.

2. Materials and methods

2.1. Study area

The study area is located in the Southeast of China and includes eight provinces in the karst region (Sichuan, Chongqing, Yunnan, Guizhou, Hunan, Hubei, Guangdong, and Guangxi). This area has a unique geological setting and high landscape heterogeneity. It is a very fragile environment. Due to a high population density and consequent land degradation, environmental problems have become increasingly severe. Moreover, it shows a continuous expansion trend in

agriculture and urban areas, representing a threat to the Yangtze River's ecological security and the Pearl river basin. The climate of the China southwestern karst region is humid and subtropical (Zhou et al., 2018). Also, agriculture and urban areas' development are increasing water demand (Lang et al., 2018). The poor regions are mainly populated by older people that are vulnerable to the high incidence of geological/geomorphological disasters (Cheng et al., 2018b). National Forestry Administration of China divided the area according to environmental conditions (e.g., geomorphology), causes of rocky desertification, and other social factors. The regions are Gorge (A), Trough valley (B), High mountain (C), Plateau (D), Fault basin (E), Plain (F), Peak cluster epikarst (G) and Hills with depressions (H). All 217 counties in this territory were classified as "poor" (The State Council Leading Group Office of Poverty Alleviation and Development, 2014) (Fig. 1).

2.2. Datasets and framework

The datasets used – NDVI, annual cumulative total precipitation, annual mean temperature, rock desertification rate, rural per capita net income (RPI), and karst control ecological engineering implementation area – and data processing are shown in Table 1. The spatial analysis of NDVI assessed the vegetation trend at the pixel level, while the other analyses were carried out at administrative unit level. The framework applied in this study is described in Fig. 2.

2.3. Methods

2.3.1. Vegetation trend

In order to assess the vegetation trend from 2000 to 2015 (NDVI) in time and space, we applied the non-parametric Theil-Median (TS) (Sen, 1968) and the Contextual the Mann-Kendall tests (CMK) (Neeti and Eastman, 2011) calculated at the pixel level. Significant correlations were considered at a $p < 0.05$. The trend is calculated according to the formula:

$$\delta = \mathrm{mean}\left(\frac{NDVI_j - NDVI_i}{j-i}\right) \quad (1)$$

where δ is the calculated trend value, and $NDVI_t$ is the NDVI value at time t ($i \le t \le j$).

2.3.2. Spatial analysis

2.3.2.1. Poverty spatial distribution and analysis. Moran's *I* was applied to measure the global spatial autocorrelation. This method was used to assess the spatial pattern of the RPI. The formula of Moran's *I* is:

$$I = \frac{n\sum_{i=1}^{n}\sum_{j=1}^{n}\omega_{ij}(x_i-\overline{x})(x_j-\overline{x})}{S\sum_{i=1}^{n}(x_i-\overline{x})^2} \quad (2)$$

where n is the number of space units, x_i is the attribute value of the ith space unit, and ω_{ij} is the value in the spatial weight matrix, so S is the sum of all the elements in the matrix. The range of Moran's *I* is [−1,1]. An index higher than 0 represent positive spatial autocorrelation (clustered pattern), while an index lower than 0 indicates a negative spatial correlation (dispersed pattern). Values close to 0 show that the variable had a random pattern.

A Hot Spot Analysis (Getis-Ord G_i^*) was applied to identify spatial poverty patterns. This tool is used to identify spatial clustering of high

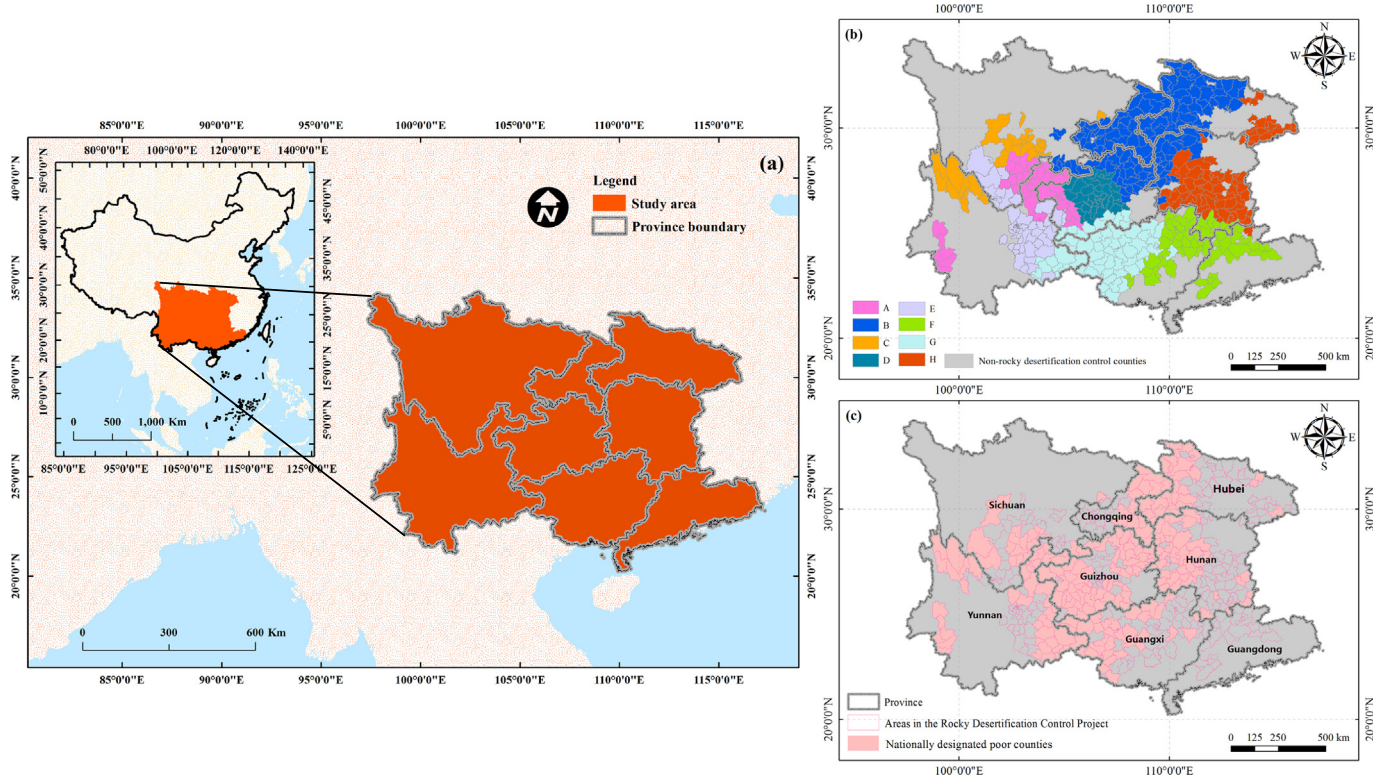

Fig. 1. (a) Location of the study area (b) Rocky desertification control counties by the NFC in southwest China. A; Gorge; B: Trough valley; C: High mountain; D: Plateau; E: Fault basin; F: Plain; G: Peak cluster epikarst; H: Hills with depressions; (c) Nationally designated poor counties (NDPC).

Table 1
Datasets used this work.

Data	Using Description	Resolution	Period	Reference	
Karst rocky desertification control counties	Counties were divided into zones of 8 rocky desertification ecological control	Counties		Derived from the documents of National Forestry grassland administration	Every zone was divided according to the *Outline of the plan for comprehensive control of rocky desertification in karst areas (2006–2015)*.
NDVI	Index from 0 to 1	1 km	2000 to 2015	Derived from the Data Center of Resources and Environmental Sciences, Chinese Academy of Sciences (http://www.resdc.cn/data.aspx?DATAID=257)	This dataset was produced based on the SPOT-VGT NDVI data (10-Day, 1 km). The annual pixel value is generated by using the Maximum Value Composite method (MVC). Annual pixel values less than 0.1 were excluded in order to present karst vegetation distribution accurately.
Annual cumulative total precipitation	Site data	Point data	2000 to 2015	Derived from National meteorological information center (http://data.cma.cn/)	Spatially using the ANUSPLIN software to interpolate into a spatial resolution of 1 km and temporal resolution of one year (covariate factor: altitude and slope) (Hijmans et al., 2005).
Annual mean temperature	Site data	Point data	2000 to 2015	Derived from National meteorological information center (http://data.cma.cn/)	Spatially using the ANUSPLIN software to interpolate into a spatial resolution of 1 km and temporal resolution of one year (covariate factor: altitude and slope) (Hijmans et al., 2005).
Rock desertification rate	Geological survey statistics showing the proportion in percentage	Counties		Derived from Institute of Karst, Chinese Academy of Geological Sciences	Using the regional geological mapping method on the basis of actual observation and analysis. The value of each county is obtained through administrative boundaries and mapping statistical data.
Rural per capita net income (RPI)	Statistical data, Statistical Yearbook of each province	Counties	2000 to 2015	Derived from Statistical Yearbook of each province (http://data.cnki.net/Yearbook/Navi?type=type&code=A)	Through the query of the province yearbook, concluded the statistical data of each county.
Karst control ecological engineering implementation area	Geological survey statistics showing the proportion in percentage	Counties		Derived from Institute of Karst, Chinese Academy of Geological Sciences	Using the regional geological mapping method on the basis of actual observation and analysis. The value of each county is obtained through administrative boundaries and mapping statistical data.

(hot) and low (cold) values with statistical significance. The formula of G_i^* is:

$$G_i^* = \frac{\sum_{j=1}^{n}\omega_{i,j}x_j - \frac{\sum_{j=1}^{n}x_j}{n}\sum_{j=1}^{n}\omega_{i,j}}{\sqrt{\frac{\sum_{j=1}^{n}x_j^2}{n} - \left(\frac{\sum_{j=1}^{n}x_j}{n}\right)^2}\sqrt{\frac{\left[n\sum_{j=1}^{n}\omega_{i,j}^2 - \left(\sum_{j=1}^{n}\omega_{i,j}\right)^2\right]}{n-1}}} \quad (3)$$

where x_j is the attribute value for year j, $\omega_{i,j}$ is the spatial weight between year i and j, and n is equal to the year's total number.

The local indicator of spatial association (LISA) was applied to identify the space-time transition. The Anselin Local Moran's *I* tool was used in local autocorrelation to identify the interdependence between the studied counties' attributes. At the same time, the cluster/outlier type (COType) field of the tool will clarify the HH, LL, HL, and LH. It is a method that shows a cluster situation every two times to identify the

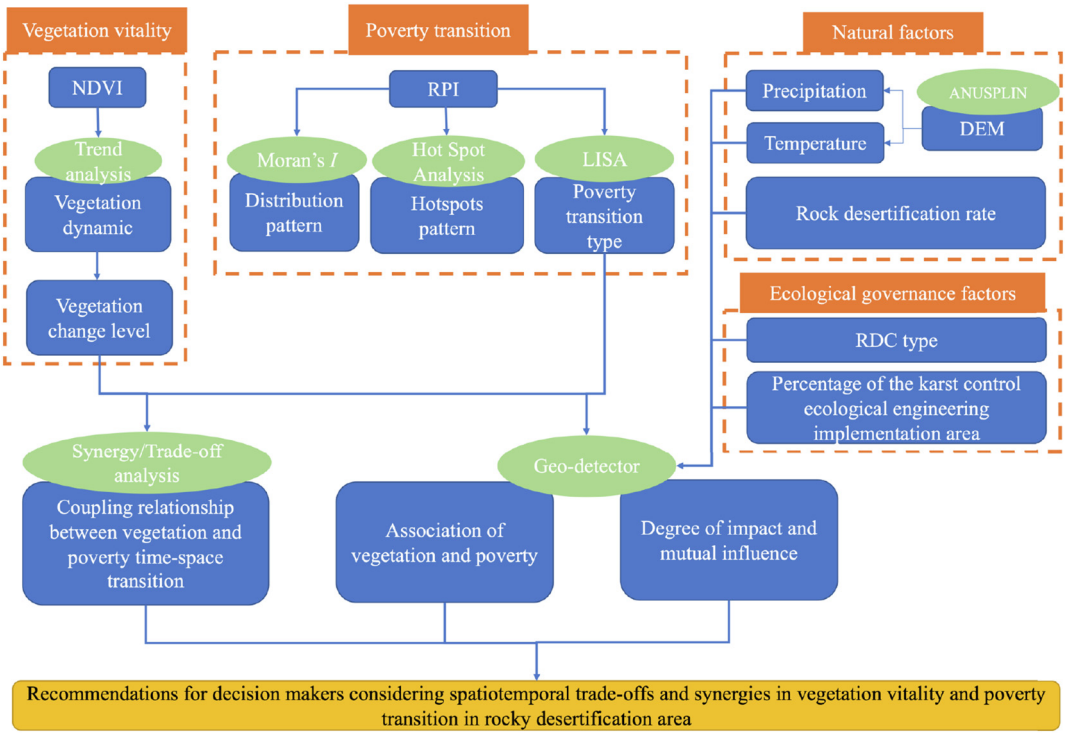

Fig. 2. Framework applied in this study.

Table 2
The types of the space-time transition. HH_t, HL_t, LL_t, LH_t represent the results of local spatial autocorrelation in each county in year t. HH: the area indicating the high value is surrounded by other areas of high value; LH: the area indicating the low value is surrounded by other areas of high value; LL: the area indicating the low value is surrounded by other areas of low value; HL: the area indicating the high value is surrounded by other areas of low value; space-time lock, flow and coagulation are sequentially expressed levels of time and space transitions. According to the situation change, the invariant, one side transformed, both sides transformed are the space-time lock, flow and coagulation, respectively.

Type	Description	Evolution	Time and space transition
$Type_0$	No transition between self and neighbors.	Invariant	Space-time lock (SL) (low level)
$Type_1$	Self-transition, neighbors no-transition.	$HH_t \rightarrow LH_{t+1}$, $HL_t \rightarrow LL_{t+1}$, $LH_t \rightarrow HH_{t+1}$, $LL_t \rightarrow HL_{t+1}$	Space-time flow (SF)
$Type_2$	Neighbors transition, self no-transition.	$HH_t \rightarrow HL_{t+1}$, $HL_t \rightarrow HH_{t+1}$, $LH_t \rightarrow LL_{t+1}$, $LL_t \rightarrow LH_{t+1}$	(middle level)
$Type_{3A}$	Self and neighbors transform in the same direction.	$HH_t \rightarrow LL_{t+1}$, $LL_t \rightarrow HH_{t+1}$	Space-time coagulation (SC)
$Type_{3B}$	Self and neighbors transform in the contrary direction.	$HL_t \rightarrow LH_{t+1}$, $LH_t \rightarrow HL_{t+1}$	(high level)

transition (Ord and Getis, 2010; Sokal et al., 1998). The space-time transition was divided into four types: $Type_0$, $Type_1$, $Type_2$, $Type_3$ (Rey and Janikas, 2006) (Table 2). Spatial analysis was carried out with ArcGIS 10.6.

2.3.2.2. Relationship between vegetation trend and poverty. Based on the rate of vegetation change in the grid, the zonal statistical tool was applied to calculate the mean NDVI at the county level. If the NDVI variability was greater than zero, we observed a greening trend. If it is lower than 0, we found a browning trend. In order to assess the degree of vegetation greening, the natural discontinuous point method was used. The levels of vegetation greening were divided into slow, stable, and quick. NDPC was divided into three categories according to the time and spatial transition of poverty: space-time lock (SL), space-time flow (SF), and space-time coagulation (SC). These represent the low, middle and high degrees/possibilities of the spatiotemporal poverty transition.

Tradeoff and synergy analysis has been used in the game research (J. Li et al., 2019; Z. Li et al., 2019; Qi et al., 2013) and ecosystem services (X. Liu et al., 2019; Y. Liu et al., 2019; Zhou et al., 2016) research to identify conflicts and benefits. A positive relation between two factors represents a synergy, while a negative relation is considered a tradeoff. (Defriez and Reuman, 2017). In this work, we assessed the relation between vegetation patterns and poverty. The degree of relation (tradeoffs and synergies) is shown in Table 3.

2.3.3. Geo-detectors: factors affecting vegetation changes

Geo-detector is a method used to detect the interaction of driving factors based on the calculation of the variance (H. Wang et al., 2019; K. Wang et al., 2019). The independent variable needs to be continuous, and the driving variables should be divided into the categories (Wang and Hu, 2012). The factor can detect not only the spatial heterogeneity of the dependent variable but also the power of the determinant of the independent variables on the dependent variable. The value is measured by the q value.

$$q = 1 - \frac{\sum_{h=1}^{L} N_h \sigma_h^2}{N\sigma^2} = 1 - \frac{SSW}{SST} \tag{4}$$

Table 3
The balance relationship in vegetation and poverty transition.

Vegetation change level	Poverty transition type	Trade-off and synergy
Browning	SL	Trade-off
	SF	Weak synergy
	SC	Strong synergy
Slowly greening	SL	Trade-off
	SF	Weak synergy
	SC	Strong synergy
Stable greening	SL	Trade-off
	SF	Weak synergy
	SC	Strong synergy
Quick greening	SL	Trade-off
	SF	Weak synergy
	SC	Strong synergy

$$SSW = \frac{\sum_{h=1}^{L} N_h \sigma^2}{N\sigma^2} \tag{5}$$

$$SST = N\sigma^2 \tag{6}$$

where h = 1, …, L is the layer of independent variable X. N_h and N are the number units in layer h and all regions, respectively. σ_h^2 and σ^2 are the variances in the layer and the variance in the region. SSW is the sum of the spatial variance in layers; SST is the total variance of Y in the region, L means the layer number. The q value is taken from 0 to 1. If factor X controls the vegetation trend, the q value is 1; if the factor X is not related to Y, the q value is 0.

The interaction detector of geo-detector is robust compared to other statistical methods in the interaction analysis. It can identify the combination of every two factors' driving degree by the q values (Wang et al., 2016). The result of the two factors interaction can be classified into five types (Table 4).

The most suitable factors are shown in Table 4. According to local characteristics, the variation of vegetation was taken as the dependent variable Y. The independent variable will be selected from the following factors (J. Li et al., 2019; Z. Li et al., 2019; Tong et al., 2018; Wang et al., 2015; Yang et al., 2017; Zhang et al., 2018): Poverty factor: The poverty transition type from 2000 to 2015 is the independent variable X_1. Annual average annual precipitation of the county is the independent variable X_2, the annual average temperature of the county is the independent variable X_3, the incidence of rocky desertification in the county is the independent variable X_4, county rocky desertification control area is the independent variable X_5. The percentage of ecological restoration per county is the independent variable X_6 (Table 4).

3. Results

3.1. Vegetation dynamic in karst national designed poor counties

TS and CMK test results showed that vegetation cover increased significantly between 2000 and 2015 in karst national designed poor counties (NDPC) and rocky desertification counties (RDC) by 81.87% and 78.77%, respectively. On the contrary, a significant decreasing trend was observed in 0.99% (NDPC) and 1.26% (RDC) ($p < 0.05$). Overall, more than 80% of the vegetation in karst NDPC was gradually greening, and no more than 1% of NDPC had a growing browning increase. However, the greening degree in RDC was lower than in NDPC, which was nearly 3%. Overall, almost no browning trend was observed in both regions. The most browning trend was observed in RDC ($p < 0.05$) and a higher percentage (19.97%) was observed in RDC, compared to NPDC (17.15%). The significant trend (both greening and browning) in vegetation vitality was higher in NPDC (82.58%) than in RDC (80.30%) ($p < 0.05$). (Figs. 3 and 4).

In the karst trough valley (B), karst plateau (D), and peak cluster epikarst (G) of NDPC regions, more than 80% area showed a greening trend (Table 5). Among all the karst NDPC regions, karst high mountains (C) are the ones with a lower greening trend and higher browning trend.

Table 4
Geo-detector layers selection.

Variable	Type/layers	Name	Instruction	The category/range
Y	Vegetation change	NDVI variation	According to the zone statistic tool to calculate the NDVI variation to represent the value of every county.	
X_1	Poverty factor	Poverty transition type	According to SL, SF, SC classification	According to the Table 2
X_2	Natural factor	Annual cumulative total precipitation	According to the zone statistic tool to calculate the average annual cumulative total precipitation to represent the value of every county. According to the result, it is made into 6 ranges.	700–900 mm, 900–1100 mm, 1100–1300 mm, 1300–1500 mm, 1500–1700 mm, 1700–1900 mm
X_3		Annual mean temperature	According to the zone statistic tool to calculate the annual mean temperature to represent the value of every county. According to the result, it is made into 6 ranges.	8 °C–11 °C, 11 °C–14 °C, 14 °C–17 °C, 17 °C–20 °C, 20 °C–22 °C
X_4		Rock desertification rate	According to geological survey statistics, the value of every county is classified into 10 ranges.	<10%, 10%–20%, 20%–30%, 30%–40%, 40%–50%, 50%–60%, 60%–70%, 70%–80%, 80%–90%, >90%
X_5	Ecological governance factor	RDC type	According to Fig. 1, it is classified into 8 categories.	A: Gorge; B: Trough valley; C: High mountain; D: Plateau; E: Fault basin; F: Plain; G: Peak cluster epikarst; H: Hills with depressions;
X_6		The percentage of the karst control ecological engineering implementation area	According to geological survey statistics, the value of every county is the ratio of the area of karst control ecological engineering implementation to the total area of the county classified into 10 categories.	<10%, 10%–20%, 20%–30%, 30%–40%, 40%–50%, 50%–60%, 60%–70%, 70%–80%, 80%–90%, >90%

3.2. Vegetation recovery with the spatiotemporal poverty distribution and transition

3.2.1. Poverty spatial distribution relationship and transition characters

Moran's *I* results for RPI in karst NDPC from 2000 to 2015 are shown in Table 6. In all the cases, poverty had a significant clustered pattern, especially in 2000 and 2001. The pattern of hot and cold spots in RPI changed between 2000 and 2015. In 2000, hotspots were concentrated in the western and northern regions and the cold spots in eastern and southern areas. In 2015, this pattern changed, and the hot spots were located, especially in the north of the study area. The cold spots were observed in the south (Fig. 5a and b).

The spatiotemporal transition in RPI can be observed in Fig. 5c, and d. The spatiotemporal transition was more evident in 2000 than in 2015. In 2000, LL and HL counties were located in the south and west. The counties with LH and HH were identified in the east and north parts. In 2015, the LL and HL were observed in the south, LH, and HH in the north.

3.2.2. Coupling relationship between vegetation and poverty time-space transition

The results showed that the relation between vegetation and poverty was variable in space. We observed synergies between vegetation and poverty transitions in most of the cases. Nevertheless, the proportion of weak synergies (42.86%) was higher than that of strong synergies (8.76%). The weak synergies between vegetation change and poverty transition type were 42.86% (browning), 45.45% (slowly greening), 43.65% (stable greening), and 37.50% (quick greening). However, a tradeoff between vegetation change and the poverty transition type was observed in 42.86% (browning), 40.91% (slowly greening), 48.41% (stable greening), and 57.50% (quick greening). Notably, only the tradeoff relationship in quick greening counties was higher than 50%. Strong synergies were observed in 14.29% (browning), 13.64% (slowly greening), 7.94% (stable greening), and 5.00% (quick greening) areas. The tradeoffs between vegetation and poverty transition in karst fault basin (E), karst plain (F), karst peak cluster epikarst (G), and karst hills with depressions (H) were higher than the synergies (Fig. 5). In the areas karst gorge (A), karst trough valley (B), karst high mountain (C), and karst plateau (D), it was observed the opposite. In the area karst fault basin (E) and karst plain (F), we did not identify a strong synergy relationship. Considering all the regions, we found 51.61% of the studied area a synergistic relationship and 48.39% a tradeoff. Nevertheless, the proportion of weak synergy (42.86%) was higher than that of strong synergy (8.76%) (Figs. 6 and 7).

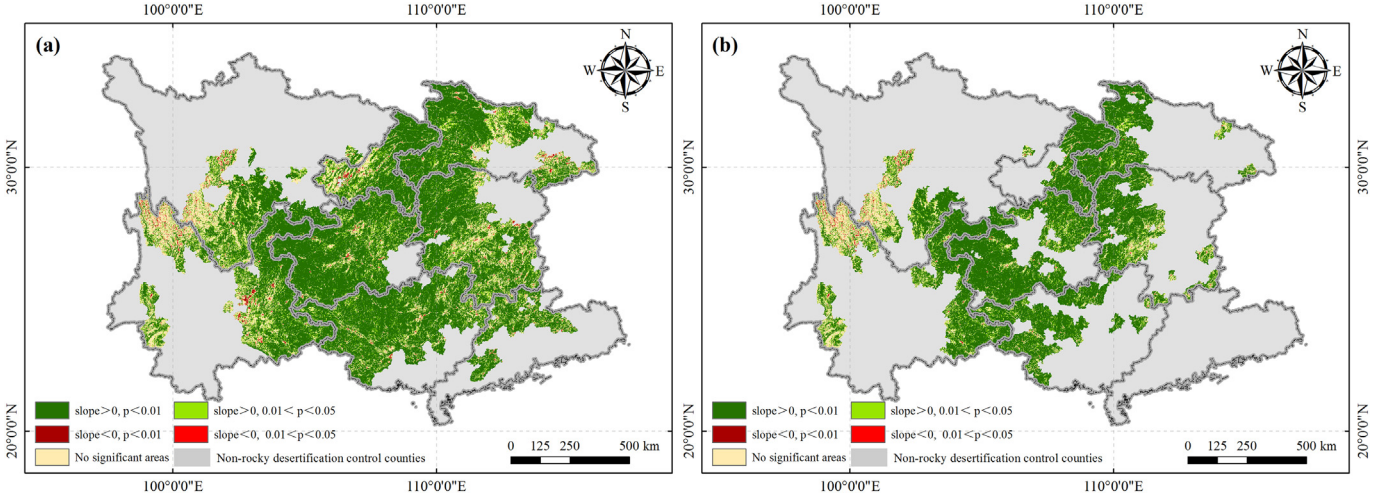

Fig. 3. Spatial NDVI trends during the period 2000–2015 in (a) RDC (b) karst NDPC in 1 km resolution. The green and the red color means the significant increasing and decreasing NDVI area, respectively. The darker green and red color indicates a *p* value less than 0.01, while the lighter indicates a p value between 0.01 and 0.05. The yellow color means no significant areas. The grey color means the non-rocky desertification control counties. (For interpretation of the references to color in this figure legend, the reader is referred to the web version of this article.)

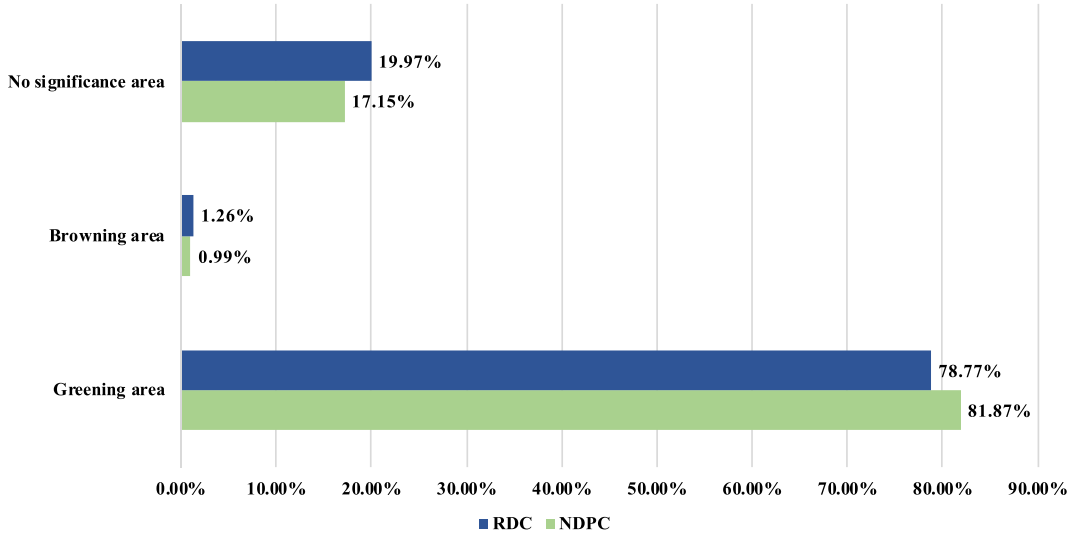

Fig. 4. Percentage of significant greening area and browning area ($p < 0.05$) in RDC and NPDC.

3.3. Geo-detectors: the association of vegetation and poverty, the degree of impact and mutual influence

The groups of factors that can affect vegetation importantly were 0.323 ($X_4 \cap X_6$, rocky desertification rate, and ecological engineering implementation area); 0.245 ($X_5 \cap X_6$, RDC type, and ecological engineering implementation area); 0.242 ($X_1 \cap X_4$, space-time poverty transition type and rocky desertification rate); 0.238 ($X_4 \cap X_5$, the rocky desertification rate, and RDC type) (Table 7).

The space-time poverty transition type (X_1) can produce a strong positive effect on the vegetation when combined with the rocky desertification rate (X_4). Among the natural factors, the rocky desertification rate (X_4) can be combined with the space-time poverty transition type (X_1), the RDC type (X_5), and the area of ecological restoration implementation (X_6) to affect the vegetation changes in a robust synergetic way. The annual average temperature and annual precipitation have little effect on vegetation changes. For the ecological governance factors, RDC type (X_5) and the area of ecological restoration implementation (X_6) can produce positive effects with X_1, X_2, X_3, and X_4.

4. Discussion

Previous works showed that China's vegetation increase contributed importantly to global greening (Chen et al., 2019; Zhu et al., 2016). Due to the afforestation, vegetation restoration, and agricultural intensification, pronounced greening has been observed in China and India (Piao et al., 2020). This is primarily a consequence of the numerous restoration programs (such as soil and water conservation, natural forest conservation and Grain for Green), which are a step toward reaching the United Nations Sustainable Development Goals (Yu et al., 2020).

The greening trend observed in our work was identified previously in the studied area (Tong et al., 2018; S. Zhao et al., 2020; R. Zhao et al., 2020). The vegetation of the karst NPDC has become significantly greener. On average, it was higher than in RDC. From 2000 to 2015, several restoration programs (fast-growing and high-yielding Timber, forest ecosystem compensation, wildlife conservation, and nature protection, the partnership to combat land degradation, rocky desertification treatment, grassland ecological protection, and cultivated land quality) were implemented in NPDC (Yang et al., 2017; Zhang et al., 2018). The Chinese government made a high investment in the area to reduce poverty (Ouyang et al., 2016) so that NPDC of the RDC area could have better results. The implementation of the same measures in different areas proved to have heterogeneous impacts due to the complex terrain and fragile ecosystem (H. Wang et al., 2019; K. Wang et al., 2019). Overall, the greening in karst NPDC is a consequence of nature and restoration programs (Tong et al., 2018).

For karst NDPC among the various RDC, karst trough valley (B), plateau (D), and peak cluster epikarst (G) areas had better results after vegetation restoration. In these regions, frequent droughts are considered a problem for vegetation development. Better management of

Table 5
Rank of the proportion of significant area in the karst NDPC vegetation dynamic in different RDC types.

Rank (high to low)	The proportion of significant greening area ($p < 0.05$)	RDC type	Rank (low to high)	The proportion of significant browning area ($p < 0.05$)	RDC type
1	83.23%	B	1	0.10%	G
2	82.95%	D	2	0.14%	B
3	82.01%	G	3	0.18%	D
4	74.20%	*A*	4	0.19%	*A*
5	67.87%	*F*	5	0.21%	*F*
6	65.77%	*H*	6	0.23%	*H*
7	58.50%	*E*	7	0.68%	*E*
8	34.45%	*C*	8	3.08%	*C*

Italicized fonts: the same order in both rankings.

Table 6
the global spatial autocorrelation results of RPI in karst NPDC.

Year	Moran's *I*	*Z*-value	*p*-Value
2000	0.260	12.636	0.000
2001	0.234	11.405	0.000
2002	0.190	9.312	0.000
2003	0.185	9.073	0.000
2004	0.173	8.493	0.000
2005	0.164	8.070	0.000
2006	0.117	5.804	0.000
2007	0.120	5.920	0.000
2008	0.131	6.434	0.000
2009	0.118	5.818	0.000
2010	0.142	6.976	0.000
2011	0.157	7.708	0.000
2012	0.157	7.698	0.000
2013	0.142	6.987	0.000
2014	0.193	9.424	0.000
2015	0.188	9.211	0.000

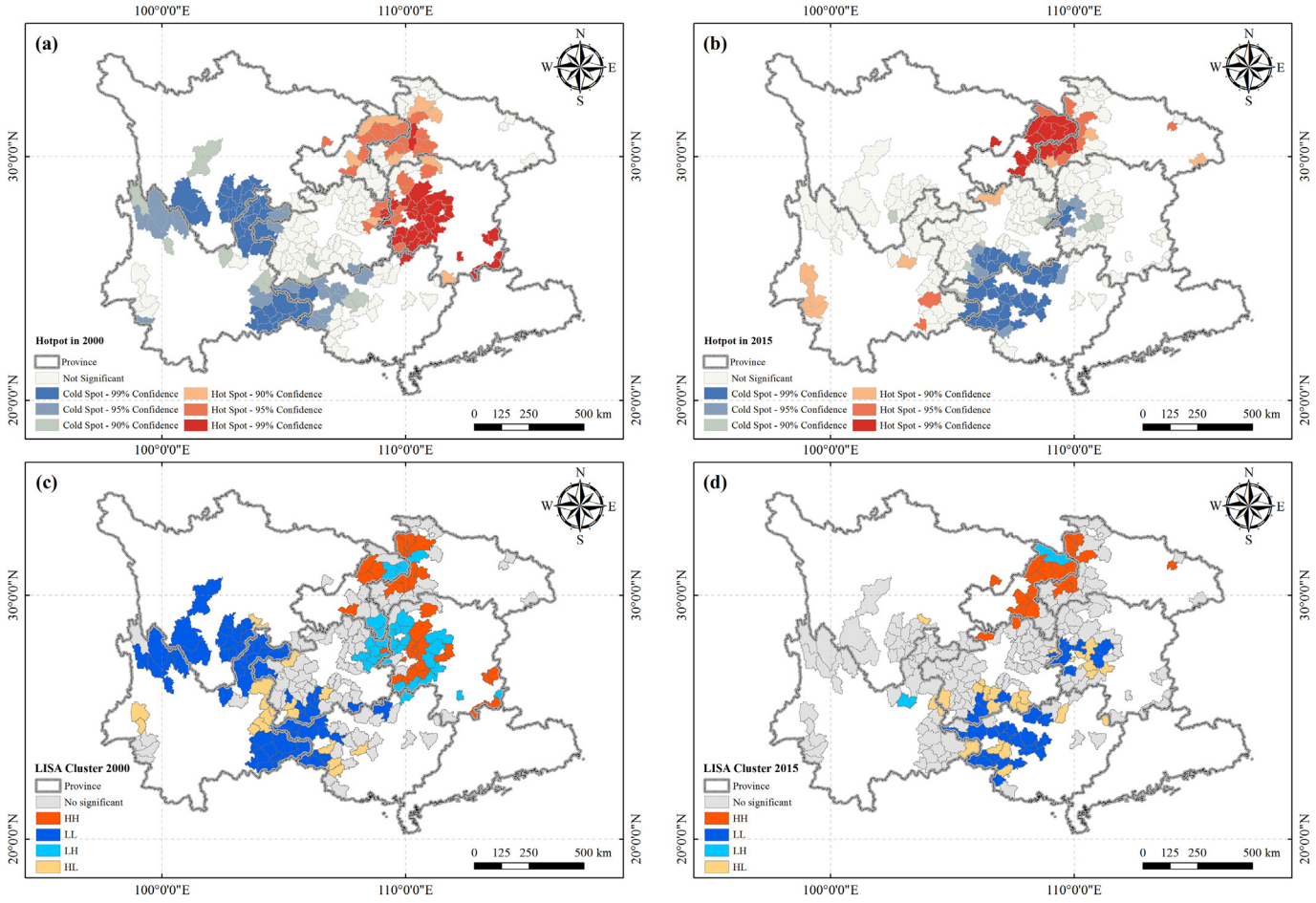

Fig. 5. Poverty hotpots (a, b) and LISA cluster ($p < 0.05$) distribution (c, d) of NPDC. The map (a) and (c) are for 2000 and the (b) and (d) are for 2015.

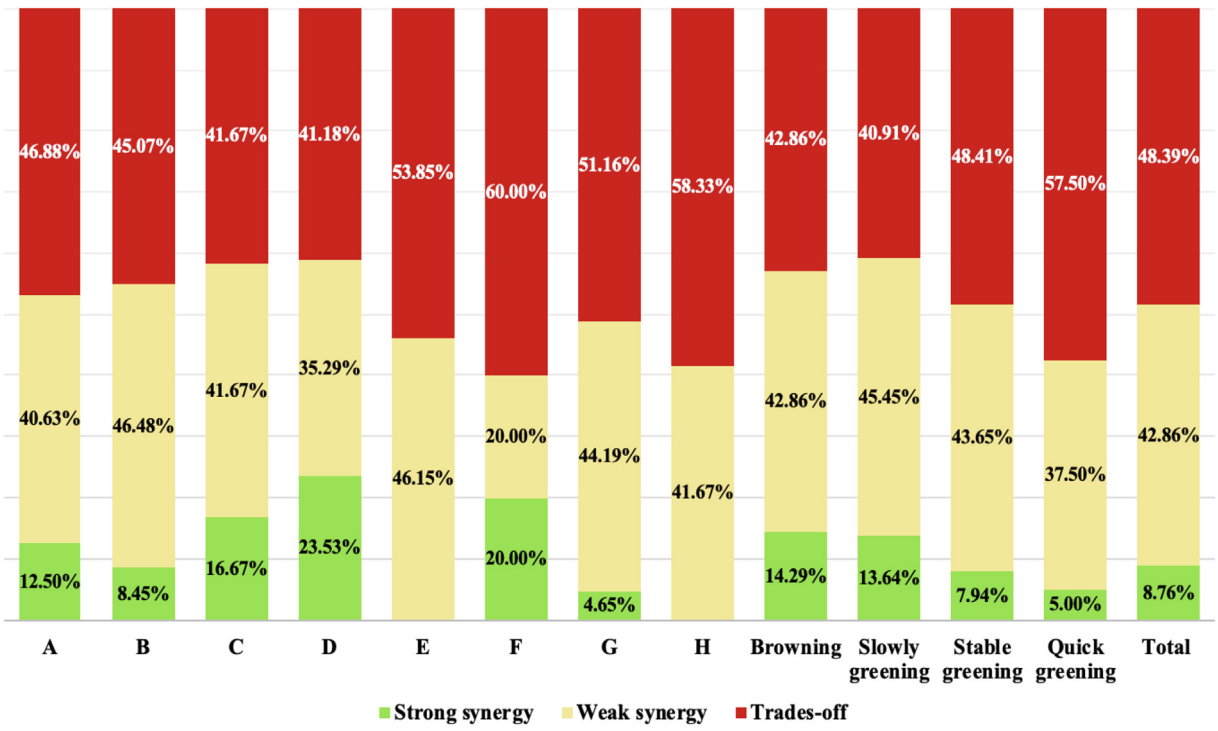

Fig. 6. Synergies and tradeoffs percentage accumulation of the relationship between vegetation change and poverty transition in karst national designed poor counties and the relationship affected by browning, slowly greening, stable greening and quick greening areas.

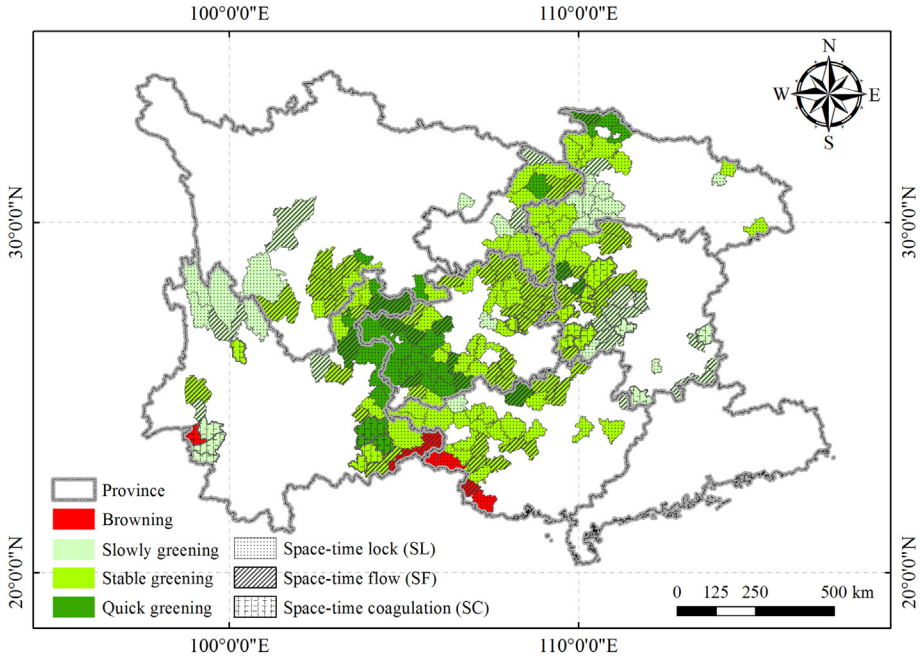

Fig. 7. Spatial distribution of various vegetation trend level and poverty transition type during 2000–2015 for the karst national poor county. The color shows the vegetation trend level (red for browning and the darkness of the green color for the degree of greening). The pattern shows the poverty transition type (Dots for SL, Slashes for SF and imaginary line mesh for SC). The overlay of color and pattern represent both the vegetation trend and the poverty transition type in every county. (For interpretation of the references to color in this figure legend, the reader is referred to the web version of this article.)

water resources and irrigation efficiency would contribute to alleviating the effects of the drought (Yang et al., 2017). So, the efficient use of water resources is a concern in the region. In some areas, terracing has been used to reduce soil and water losses (H. Wang et al., 2019; K. Wang et al., 2019). On the other hand, restoration of vegetation in the high mountain (C) and fault basin (E) was less successful. In the fault basin, soil and water storage are more difficult, affecting vegetation recovery (Zhou et al., 2020). Previous works highlighted that vegetation restoration practices is not the only solution for all areas (Bryan et al., 2018). This shows that the restoration measures should be more detailed in the study area and applied according to the environmental characteristics. Other measures, such as ecological and engineering control measures could be considered to restore vegetation in karst rocky desertification area in China.

Table 7
The dominant interactions between two covariates on vegetation trends.

Interaction	Degree of the relationship (q)
Poverty transition ∩ Precipitation	0.060
Poverty transition ∩ Temperature	0.055
Poverty transition ∩ Rock desertification rate	**0.242**
Poverty transition ∩ RDC type	0.046
Poverty transition ∩ Ecological engineering implementation area	0.120
Precipitation ∩Temperature	0.099
Precipitation ∩ Rock desertification rate	0.165
Precipitation ∩ RDC type	0.133
Precipitation ∩ Ecological engineering implementation area	0.154
Temperature ∩ Rock desertification rate	0.196
Temperature ∩ RDC type	0.131
Temperature ∩ Ecological engineering implementation area	0.125
Rock desertification rate ∩ RDC type	**0.238**
Rock desertification rate ∩ Ecological engineering implementation area	**0.323**
RDC type ∩ Ecological engineering implementation area	**0.245**

Poverty transition∩ RDC type is Bi-factor enhancement and others are the Nonlinear enhancement. Bold and underlined front is the q value at the top.

The spatiotemporal poverty distribution in karst NPDC changed from 2000 to 2015, showing that RPI was not stable. This may be attributed to the delay in responding to the implemented measures. Society responds differently to the same measures and the greening trend. Also, poverty is influenced by many variables, not all related to vegetation restoration (Cao et al., 2014).

The change of spatiotemporal poverty transition pattern in karst NPDC from 2000 to 2015 showed that the poverty reasons also changed. Vegetation restoration was an opportunity for poverty alleviation and wellbeing improvement. Relocating population to settlements reduced poverty (Cao et al., 2009). In Guizhou province, the authorities relocated the population and planted trees to alleviate poverty (Cheng et al., 2017). This measure decreased rural population poverty and the pressures on vulnerable karst areas (Yang et al., 2020). Also, the relocation of the population contributed to vegetation reestablishment in rural areas (Cao et al., 2014; H. Wang et al., 2019; K. Wang et al., 2019).

In the quick greening area, the vegetation change and the poverty transition had a tradeoff relationship. However, synergies were identified in a not so quick greening area. From this, it can be observed that the rapid growth of vegetation did not improve poverty alleviation. Therefore, the vegetation growth resulted from the control of rocky desertification did not increase human wellbeing. Also, no strong synergy was observed in the counties located in the fault basin (E) and hills with depressions (H). This means that the vegetation improvement in these two areas did not change the poverty status as well. The harsh natural conditions (e.g., sinkholes) and the high vulnerability to floods and landslides, in fault basin (E) and hills with depressions (H), made vegetation restoration not so effective as in other areas. The reduced natural capacity for the soils to store water reduced the effectiveness of the restoration measures (Gutiérrez et al., 2014; Zhou et al., 2018). The poor natural conditions influence the residents' farming, land quality, water supply, and other basic productions and living conditions. This decreases the region and poverty transition. Therefore, poverty alleviation in karst NDPC is not only related to the vegetation greening but also the RDC type.

The results showed that high mountain (C), Plain (F), and Plateau (D) are the main areas of strong synergy between vegetation change

degree and poverty transition. This means that the relationship between vegetation change and poverty transition in these areas of the RDC is higher than in other areas. Compared with other regions, the altitude in Plateau (D) and High mountain (C) is variable with the complex terrain, which results in the microclimates and diverse vegetation types. Restoration measures and the availability of resources decreased population poverty (Cao et al., 2009). In the Plain (F) area, agriculture development increased population income and reduced poverty. Therefore, vegetation development (by restoration and crops) was vital for poverty alleviation in the RDC. Ecological restoration improved vegetation coverage, water conservation, and reduced the exposition to natural disasters (Liao et al., 2018). In fact, the fragile karst ecosystem associated with high human pressure is a cause of natural disasters and poverty in southwestern China's karst areas (Wang et al., 2004). Fortunately, we found a synergy between karst NPDC vegetation and the poverty transition. On this basis, the measures applied were beneficial for agriculture development, promote transportation, improve education, and ultimately ensure people's cultural level and spiritual abundance. Geo-detector analysis highlighted that the interaction between the rocky desertification rate and poverty transition type ($X_1 \cap X_4$) is relevant and can influence the vegetation. In this work, the poverty transition type factor was important for vegetation dynamics in RDC. Geographic conditions influence household productivity (Jalan and Ravallion, 2002). In the karst NPDC, the rocky desertification rate affected vegetation development and land productivity. Therefore, natural factors are responsible for poverty (Jiang et al., 2014). The most determinant factor for karst vegetation is the interaction of rocky desertification rate and area of ecological restoration ($X_4 \cap X_6$). This is a consequence of natural factors and environmental governance options. Ecological restoration measures prevented the rocky desertification, which was beneficial for the environment and population living in NPDC. Overall, the rocky desertification rate (X_4) can interact with the poverty transition (X_1), RDC type (X_5), and the area of ecological engineering implementation (X_6). This makes rocky desertification rate (X_4) an important active factor. Rocky desertification is a barrier for the vegetation establishment. It also influences the socio-economic development of the area and the restoration measures implemented (J.Y. Zhang et al., 2016).

The interaction of RDC type and ecological engineering implementation ($X_5 \cap X_6$) highlighted the importance of governance factors. Overall, the rocky desertification rate (X_4) and the ecological governance factors (X_5 and X_6) should be the next concerns for vegetation restoration in karst NPDC. The ecological governance factor increased the interaction with other factors, showing that restoration measures are essential for the greening trend. It is crucial to reduce desertification and increase the resilience of the studied area to natural disasters (Liao et al., 2018; Tong et al., 2018). Implementing environmental management in the rocky desertification area is in line with the local natural and social background and has positive implications. Successful measures need to consider the environmental and social conditions of the area. Weak measures such as unsuitable species selection and low compensation rates for peasants may undermine restoration programs (Tong et al., 2017).

Vegetation restoration can improve poverty alleviation. This synergy contributes to the wellbeing of the local communities. How to balance the poverty alleviation measures and ecology recovery will be the next critical problem in rural karst area in southwest China (Cheng et al., 2018b; Fisher et al., 2014; J. Zhang et al., 2016). This study's results are relevant for policy-making since we identified the areas where vegetation restoration has positive or no impacts on poverty alleviation. This information will be useful to improve population wellbeing. Overall, several studies highlighted that restoration measures improved environmental quality (e.g., Peng et al., 2011; Liu et al., 2014), ecosystem health (Liao et al., 2018), ecosystem services provisioning (Tian et al., 2016) and households livelihood diversity (J. Zhang et al., 2016) of southwest China karst region. Nevertheless, human management and climate conditions, also local realities, need to be considered in the measures (Tong et al., 2017), in order to avoid conflicts, although the population in this region is more aware of environmental problems, especially related to land and water management (Oliver et al., 2020). Different restoration practices are needed in areas where the vegetation restoration was not so effective in reducing poverty (e.g., high mountain and fault basin). The limited environmental conditions did not allow restoration practices to reduce poverty in these areas. Therefore, future policies should be tailored to tackle poverty in such areas. Measures such as subsidies, compensations, tax reductions could be established. Synergies and tradeoffs analysis were crucial to understanding the complex relations between vegetation restoration and poverty alleviation. Therefore, for policy-making, these analyses could be considered before design or implement plans or strategies. On the global scale, achieving the United Nations (poverty reduction, vegetation recovery, and wellbeing promotion), spatiotemporal tradeoffs, and synergies in vegetation vitality and poverty transition in a rocky desertification area will be the next step (Administration, 2018). The enacted further development policy efforts can be the pathways to sustainable development and poverty eradication (UNEP, 2011). However, we should not ignore the completion of the policy and the effectiveness test for a long time to ensure the policy power (Crespo Cuaresma et al., 2018). In the human-land developing progress, the frequency of harsh conflicts in NPDC hamper the possibility for the development of a sustainable plan for future land management. Furthermore, the solution should come from considering the vegetation and poverty and the ecology-development balance. Therefore, ecological and environmental degradation and poverty must be tackled together to achieve the win-win strategies on local and national levels (Cheng et al., 2018a).

Modeling exercises have limitations and uncertainties. In this work, we tried to tackle this by selecting the best resolution data and data from official sources. Data availability is one of the most common barriers to developing high-resolution studies (e.g., Shay et al., 2016; Rova et al., 2018; Inacio et al., 2020). The period of analysis was between 2000 and 2015. Unfortunately, for the studied area, there was not more recent data than 2015. We acknowledge the necessity of more updated data, and this will be more relevant and would strengthen and make more actual our analysis and proposals for the management of NPDC. Nevertheless, we studied a robust period (2000–2015), and the conclusions obtained from this work are trustworthy. We are aware that the NDVI resolution (1 km^2) overlooks fine-scale details and is not appropriate to local level studies. However, for the spatial scale of this work (regional), it provides satisfactory results. Another limitation and source of uncertainty was the fact that point data (Annual cumulative total precipitation and Annual mean temperature) was interpolated, and there are always errors (e.g., Bier and Godoy de Souza, 2017; Jain and Flannigan, 2017; Garcia-Santos et al., 2020). In our study, to be aligned with NDVI data, the pixel resolution was 1 km^2. Therefore, at a local level, the generalization can be high. The resolution of socio-economic data (e.g., Rock desertification rate, RPI) is coarser, which increases the generalization when compared to biophysical data (e.g., NDVI). In this case, we have only a general idea of each county but cannot understand the heterogeneities at a finer scale. This is a significant limitation and can produce some uncertainties in the analysis at the county level. In the process of performing spatial assessments (e.g., hotspot, LISA), assessing synergies and tradeoff, and geodetector analysis, all the data were analyzed at the county scale (including NDVI, Annual cumulative total precipitation, and Annual mean temperature, losing even more detail). The values in each county correspond to the average value to be comparable. This also increase the error of the analysis. Similar obstacles were identified also in previous works that assessed data with different spatial resolutions (e.g., Immitzer et al., 2018; Räsänen and Virtanen, 2019; Pastén-Zapata et al., 2020). Despite the limitations and uncertainties observed, we consider that our work is significant to decision-making and contribute to understanding the factors involved in vegetation restoration and poverty transition.

5. Conclusion

In the karst NPDC of southwest China, the vegetation restoration effect was more evident than other RDC areas. This is an evidence that vegetation recuperation reduced poverty levels. In most cases of vegetation growth, there were synergies with poverty alleviation. However, in situations where vegetation grows quickly, there is a tradeoff relationship with poverty alleviation. The vegetation in the areas where this occurs is mainly influenced by the interaction of the rocky desertification rate and ecological restoration. The poverty transition type can also substantially impact the rocky desertification rate and affect vegetation changes. The rocky desertification rate can influence the vegetation changes in a strong synergy with the space-time poverty transition type, the RDC type, and the area of ecological restoration implementation. The poverty alleviation can impact on vegetation recovery positively. We should pay more attention to land management to maintain the sustainability of the human-ecological system.

CRediT authorship contribution statement

Sen Zhao: Conceptualization, Methodology, Software, Writing - original draft, Visualization, Writing - review & editing, Formal analysis. **Xiuqin Wu:** Conceptualization, Writing - review & editing, Project administration, Data curation. **Jinxing Zhou:** Supervision, Project administration. **Paulo Pereira:** Conceptualization, Visualization, Writing - review & editing.

Declaration of competing interest

The authors declare that they have no known competing financial interests or personal relationships that could have appeared to influence the work reported in this paper.

Acknowledgments

This work was supported by funding from the National Natural Science Foundation of China (41671080) and the National Key Research and Development Program of China (2016YFC0502506). We are grateful to our colleagues for their insightful comments on our earlier version of this manuscript. We gratefully acknowledge the Beijing Municipal Education Commission for their financial support through Innovative Transdisciplinary Program “Ecological Restoration Engineering”. We would also like to thank experts who offered their knowledge and time commitment for this research.

Appendix A. Supplementary data

Supplementary data to this article can be found online at https://doi.org/10.1016/j.scitotenv.2020.141770.

References

Administration, N.F. and G, 2018. Bulletin on Rocky Desertification in Karst Areas of China.

Bennett, E.M., Peterson, G.D., Gordon, L.J., 2009. Understanding relationships among multiple ecosystem services. Ecol. Lett. 12, 1394–1404. https://doi.org/10.1111/j.1461-0248.2009.01387.x.

Bier, V.A., Godoy de Souza, E., 2017. Interpolation selection index for delineation of thematic maps. Comput. Electron. Agric. 136, 202–209. https://doi.org/10.1016/j.compag.2017.03.008.

Bryan, B.A., Gao, L., Ye, Y., Sun, X., Connor, J.D., Crossman, N.D., 2018. China's response to a national land-system sustainability emergency. Nature https://doi.org/10.1038/s41586-018-0280-2.

Cai, J., Huang, B., Song, Y., 2017. Using multi-source geospatial big data to identify the structure of polycentric cities. Remote Sens. Environ. 202, 210–221. https://doi.org/10.1016/j.rse.2017.06.039.

Cao, S., Zhong, B., Yue, H., Zeng, H., Zeng, J., 2009. Development and testing of a sustainable environmental restoration policy on eradicating the poverty trap in China's Changting County. Proc. Natl. Acad. Sci. 106, 10712–10716. https://doi.org/10.1073/pnas.0900197106.

Cao, S., Ma, H., Yuan, W., Wang, X., 2014. Interaction of ecological and social factors affects vegetation recovery in China. Biol. Conserv. 180, 270–277. https://doi.org/10.1016/j.biocon.2014.10.009.

Chen, C., Park, T., Wang, X., Piao, S., Xu, B., Chaturvedi, R.K., Fuchs, R., Brovkin, V., Ciais, P., Fensholt, R., Tømmervik, H., Bala, G., Zhu, Z., Nemani, R.R., Myneni, R.B., 2019. China and India lead in greening of the world through land-use management. Nat. Sustain. 2, 122–129. https://doi.org/10.1038/s41893-019-0220-7.

Cheng, F., Lu, H., Ren, H., Zhou, L., Zhang, L., Li, J., Lu, X., Huang, D., Zhao, D., 2017. Integrated emergy and economic evaluation of three typical rocky desertification control modes in karst areas of Guizhou Province, China. J. Clean. Prod. 161, 1104–1128. https://doi.org/10.1016/j.jclepro.2017.05.065.

Cheng, X., Shuai, C., Liu, J., Wang, J., Liu, Y., Li, W., Shuai, J., 2018a. Topic modelling of ecology, environment and poverty nexus: an integrated framework. Agric. Ecosyst. Environ. 267, 1–14. https://doi.org/10.1016/j.agee.2018.07.022.

Cheng, X., Shuai, C. min, Wang, J., Li, W. jing, Shuai, J., Liu, Y., 2018b. Building a sustainable development model for China's poverty-stricken reservoir regions based on system dynamics. J. Clean. Prod. 176, 535–554. https://doi.org/10.1016/j.jclepro.2017.12.068.

Crespo Cuaresma, J., Fengler, W., Kharas, H., Bekhtiar, K., Brottrager, M., Hofer, M., 2018. Will the sustainable development goals be fulfilled? Assessing present and future global poverty. Palgrave Commun 4. https://doi.org/10.1057/s41599-018-0083-y.

Defriez, E.J., Reuman, D.C., 2017. A global geography of synchrony for terrestrial vegetation. Glob. Ecol. Biogeogr. 26, 878–888. https://doi.org/10.1111/geb.12595.

Desmond, C., 2017. The ecology of rural poverty. Nat. Ecol. Evol. 1, 1060–1061. https://doi.org/10.1038/s41559-017-0251-2.

Dinda, S., 2004. Environmental Kuznets curve hypothesis: a survey. Ecol. Econ. 49, 431–455. https://doi.org/10.1016/j.ecolecon.2004.02.011.

Ezio, B., Benedetta, C., Ugo, S., 1999. Agriculture landscape and human impact in some karst of Italy. Int. J. Speleol. 28, 33–54. https://doi.org/10.5038/1827-806X.28.1.3.

Fisher, J.A., Patenaude, G., Giri, K., Lewis, K., Meir, P., Pinho, P., Rounsevell, M.D.A., Williams, M., 2014. Understanding the relationships between ecosystem services and poverty alleviation: a conceptual framework. Ecosyst. Serv. 7, 34–45. https://doi.org/10.1016/j.ecoser.2013.08.002.

Ford, D., Williams, P., 2007. Karst hydrogeology and geomorphology. Karst Hydrogeology and Geomorphology, 2nd ed. John Wiley & Sons Ltd., West Sussex, England https://doi.org/10.1002/9781118684986.

Gams, I., Gabrovec, M., 1999. Land use and human impact in the Dinaric karst. Int. J. Speleol. 28, 55–70. https://doi.org/10.5038/1827-806X.28.1.4.

Gao, J., Wang, H., 2019. Temporal analysis on quantitative attribution of karst soil erosion: a case study of a peak-cluster depression basin in Southwest China. Catena 172, 369–377. https://doi.org/10.1016/j.catena.2018.08.035.

Garcia-Santos, G., Scheiber, M., Pilz, J., 2020. Spatial interpolation methods to predict airborne pesticide drift deposits on soils using knapsack sprayers. Chemosphere 258, 127231. https://doi.org/10.1016/j.chemosphere.2020.127231.

Gutiérrez, F., Parise, M., De Waele, J., Jourde, H., 2014. A review on natural and human-induced geohazards and impacts in karst. Earth-Science Rev 138, 61–88. https://doi.org/10.1016/j.earscirev.2014.08.002.

He, J., Pan, Z., Liu, D., Guo, X., 2019. Exploring the regional differences of ecosystem health and its driving factors in China. Sci. Total Environ. 673, 553–564. https://doi.org/10.1016/j.scitotenv.2019.03.465.

Hijmans, R.J., Cameron, S.E., Parra, J.L., Jones, P.G., Jarvis, A., 2005. Very high resolution interpolated climate surfaces for global land areas. Int. J. Climatol. 25, 1965–1978. https://doi.org/10.1002/joc.1276.

Immitzer, M., Böck, S., Einzmann, K., Vuolo, F., Pinnel, N., Wallner, A., Atzberger, C., 2018. Fractional cover mapping of spruce and pine at 1 ha resolution combining very high and medium spatial resolution satellite imagery. Remote Sens. Environ. 204, 690–703. https://doi.org/10.1016/j.rse.2017.09.031.

Inacio, M., Miksa, K., Kalinauskas, M., Pereira, P., 2020. Mapping wild seafood potential, supply, flow and demand in Lithuania. Sci. Total Environ. 718, 137356. https://doi.org/10.1016/j.scitotenv.2020.137356.

Jain, P., Flannigan, M.D., 2017. Comparison of methods for spatial interpolation of fire weather in Alberta, Canada. Can. J. For. Res. 47, 1646–1658. https://doi.org/10.1139/cjfr-2017-0101.

Jalan, J., Ravallion, M., 2002. Geographic poverty traps? A micro model of consumption growth in rural China. J. Appl. Econ. 17, 329–346. https://doi.org/10.1002/jae.645.

Jiang, Z., Lian, Y., Qin, X., 2014. Rocky desertification in Southwest China: impacts, causes, and restoration. Earth-Science Rev. 132, 1–12. https://doi.org/10.1016/j.earscirev.2014.01.005.

Lang, Y., Song, W., Deng, X., 2018. Projected land use changes impacts on water yields in the karst mountain areas of China. Phys. Chem. Earth 104, 66–75. https://doi.org/10.1016/j.pce.2017.11.001.

Li, J., Xu, C., Chen, M., Sun, W., 2019a. Balanced development: nature environment and economic and social power in China. J. Clean. Prod. 210, 181–189. https://doi.org/10.1016/j.jclepro.2018.10.293.

Li, Z., Xu, X., Zhang, Y., Wang, K., Zeng, P., 2019b. Reconstructing recent changes in sediment yields from a typical karst watershed in southwest China. Agric. Ecosyst. Environ. 269, 62–70. https://doi.org/10.1016/j.agee.2018.09.024.

Liao, C., Yue, Y., Wang, K., Fensholt, R., Tong, X., Brandt, M., 2018. Ecological restoration enhances ecosystem health in the karst regions of southwest China. Ecol. Indic. 90, 416–425. https://doi.org/10.1016/j.ecolind.2018.03.036.

Liu, Y., Huang, X., Yang, H., Zhong, T., 2014. Environmental effects of land-use/cover change caused by urbanization and policies in Southwest China Karst area – a case study of Guiyang. Habitat Int 44, 339–348. https://doi.org/10.1016/j.habitatint.2014.07.009.

Liu, Y., Li, Y., Li, S., Motesharrei, S., 2015. Spatial and temporal patterns of global NDVI trends: correlations with climate and human factors. Remote Sens. 7, 13233–13250. https://doi.org/10.3390/rs71013233.

Liu, H., Zhang, M., Lin, Z., Xu, X., 2018. Spatial heterogeneity of the relationship between vegetation dynamics and climate change and their driving forces at multiple time scales in Southwest China. Agric. For. Meteorol. 256–257, 10–21. https://doi.org/10.1016/j.agrformet.2018.02.015.

Liu, X., Blackburn, T.M., Song, T., Li, X., Huang, C., Li, Y., 2019a. Risks of biological invasion on the belt and road. Curr. Biol. 29, 499–505.e4. https://doi.org/10.1016/j.cub.2018.12.036.

Liu, Y., Lü, Y., Fu, B., Harris, P., Wu, L., 2019b. Quantifying the spatio-temporal drivers of planned vegetation restoration on ecosystem services at a regional scale. Sci. Total Environ. 650, 1029–1040. https://doi.org/10.1016/j.scitotenv.2018.09.082.

Montalvo, J.G., Ravallion, M., 2010. The pattern of growth and poverty reduction in China. J. Comp. Econ. 38, 2–16. https://doi.org/10.1016/j.jce.2009.10.005.

Moser, C.O.N., 1998. The asset vulnerability framework: reassessing urban poverty reduction strategies. World Dev. 26, 1–19. https://doi.org/10.1016/S0305-750X(97)10015-8.

Neeti, N., Eastman, J.R., 2011. A contextual Mann-Kendall approach for the assessment of trend significance in image time series. Trans. GIS 15, 599–611. https://doi.org/10.1111/j.1467-9671.2011.01280.x.

Oliver, D.M., Zheng, Y., Naylor, L.A., Murtagh, M., Waldron, S., Peng, T., 2020. How does smallholder farming practice and environmental awareness vary across village communities in the karst terrain of southwest China? Agric. Ecosyst. Environ. 288, 2020. https://doi.org/10.1016/j.agee.2019.106715.

Ord, J.K., Getis, A., 2010. Local spatial autocorrelation statistics: distributional issues and an application. Geogr. Anal. 27, 286–306. https://doi.org/10.1111/j.1538-4632.1995.tb00912.x.

Ouyang, Z., Zheng, H., Xiao, Y., Polasky, S., Liu, J., Xu, W., Wang, Q., Zhang, L., Xiao, Y., Rao, E., Jiang, L., Lu, F., Wang, X., Yang, G., Gong, S., Wu, B., Zeng, Y., Yang, W., Daily, G.C., 2016. Improvements in ecosystem services from investments in natural capital. Science (80-.) 352, 1455–1459. https://doi.org/10.1126/science.aaf2295.

Pang, D., Cao, J., Dan, X., Guan, Y., Peng, X., Cui, M., Wu, X., Zhou, J., 2018. Recovery approach affects soil quality in fragile karst ecosystems of southwest China: implications for vegetation restoration. Ecol. Eng. 123, 151–160. https://doi.org/10.1016/j.ecoleng.2018.09.001.

Pardo-Igúzquiza, E., Durán-Valsero, J.J., Dowd, P.A., Guardiola-Albert, C., Liñan-Baena, C., Robledo-Ardila, P.A., 2012. Estimation of spatio-temporal recharge of aquifers in mountainous karst terrains: application to Sierra de las Nieves (Spain). J. Hydrol. 470–471, 124–137. https://doi.org/10.1016/j.jhydrol.2012.08.042.

Pastén-Zapata, E., Jones, J.M., Moggridge, H.L., Widmann, M., 2020. Evaluation of the performance of Euro-CORDEX Regional Climate Models for assessing hydrological climate change impacts in Great Britain: a comparison of different spatial resolutions and quantile mapping bias correction methods. J. Hydrol. 584, 124653. https://doi.org/10.1016/j.jhydrol.2020.124653.

Peng, J., Xu, Y.Q., Cai, Y.L., Xiao, H.L., 2011. The role of policies in land use/cover change since the 1970s in ecologically fragile karst areas of Southwest China: a case study on the Maotiaohe watershed. Environ. Sci. Pol. 14, 408–418. https://doi.org/10.1016/j.envsci.2011.03.009.

Pettorelli, N., Vik, J.O., Mysterud, A., Gaillard, J.M., Tucker, C.J., Stenseth, N.C., 2005. Using the satellite-derived NDVI to assess ecological responses to environmental change. Trends Ecol. Evol. 20, 503–510. https://doi.org/10.1016/j.tree.2005.05.011.

Piao, S., Wang, X., Park, T., Chen, C., Lian, X., He, Y., Bjerke, J.W., Chen, A., Ciais, P., Tømmervik, H., Nemani, R.R., Myneni, R.B., 2020. Characteristics, drivers and feedbacks of global greening. Nat. Rev. Earth Environ. 1, 14–27. https://doi.org/10.1038/s43017-019-0001-x.

Qi, X., Ye, S., Cheng, Y., Lin, R., 2013. The game analysis between poverty and environment in ecologically fragile zones. Acta Ecol. Sin. 33, 6411–6417. https://doi.org/10.5846/stxb201304300876.

Räsänen, A., Virtanen, T., 2019. Data and resolution requirements in mapping vegetation in spatially heterogeneous landscapes. Remote Sens. Environ. 230, 111207. https://doi.org/10.1016/j.rse.2019.05.026.

Ravallion, M., Chen, S., 2019. Global poverty measurement when relative income matters. J. Public Econ. 177, 104046. https://doi.org/10.1016/j.jpubeco.2019.07.005.

Rey, S.J., Janikas, M.V., 2006. STARS: space-time analysis of regional systems. Geogr. Anal. 38, 67–86. https://doi.org/10.1111/j.0016-7363.2005.00675.x.

Rova, S., Pastres, R., Zucchetta, M., Pravoni, F., 2018. Ecosystem services' mapping in data-poor coastal areas: which are the monitoring priorities? Ocean Coast. Manag. 153, 168–175. https://doi.org/10.1016/j.ocecoaman.2017.11.021.

Schirpke, U., Candiago, S., Egarter Vigl, L., Jäger, H., Labadini, A., Marsoner, T., Meisch, C., Tasser, E., Tappeiner, U., 2019. Integrating supply, flow and demand to enhance the understanding of interactions among multiple ecosystem services. Sci. Total Environ. 651, 928–941. https://doi.org/10.1016/j.scitotenv.2018.09.235.

Sen, P.K., 1968. Estimates of the regression coefficient based on Kendall's tau. J. Am. Stat. Assoc. 63, 1379–1389. https://doi.org/10.1080/01621459.1968.10480934.

Shay, E., Combs, T.S., Findley, D., Kolosns, C., Madeley, M., Salvsen, D., 2016. Identifying transportation disadvantage: mixed-methods analysis combining GIS mapping with qualitative data. Transp. Policy 48, 129–138. https://doi.org/10.1016/j.tranpol.2016.03.002.

Smith, N.G., Keenan, T.F., Colin Prentice, I., Wang, H., Wright, I.J., Niinemets, Ü., Crous, K.Y., Domingues, T.F., Guerrieri, R., Yoko Ishida, F., Kattge, J., Kruger, E.L., Maire, V., Rogers, A., Serbin, S.P., Tarvainen, L., Togashi, H.F., Townsend, P.A., Wang, M., Weerasinghe, L.K., Zhou, S.X., 2019. Global photosynthetic capacity is optimized to the environment. Ecol. Lett. 22, 506–517. https://doi.org/10.1111/ele.13210.

Sokal, R.R., Oden, N.L., Thomson, B.A., 1998. Local spatial autocorrelation in biological variables. Biol. J. Linn. Soc. 65, 41–62. https://doi.org/10.1006/bijl.1998.0238.

Song, X.-P., Hansen, M.C., Stehman, S.V., Potapov, P.V., Tyukavina, A., Vermote, E.F., Townshend, J.R., 2018. Global land change from 1982 to 2016. Nature https://doi.org/10.1038/s41586-018-0411-9.

Su, Y., Li, T., Cheng, S., Wang, X., 2020. Spatial distribution exploration and driving factor identi fi cation for soil salinisation based on geodetector models in coastal area. Ecol. Eng. 156, 105961. https://doi.org/10.1016/j.ecoleng.2020.105961.

Tallis, H.M., Kareiva, P., 2006. Shaping global environmental decisions using socio-ecological models. Trends Ecol. Evol. 21, 562–568. https://doi.org/10.1016/j.tree.2006.07.009.

Tallis, H., Kareiva, P., Marvier, M., Chang, A., 2008. An ecosystem services framework to support both practical conservation and economic development. Proc. Natl. Acad. Sci. 105, 9457–9464. https://doi.org/10.1073/pnas.0705797105.

The State Council Leading Group Office of Poverty Alleviation and Development, 2014. A List of 832 Poverty-stricken Counties.

Tian, Y., Wang, S., Bai, X., Luo, G., Xu, Y., 2016. Tradeoffs among ecosystem services in a typical Karst watershed, SW China. Sci. Total Environ. 566-567, 1297–1308. https://doi.org/10.1016/j.scitotenv.2016.05.190.

Tong, X., Wang, K., Yue, Y., Brandt, M., Liu, B., Zhang, C., Liao, C., Fensholt, R., 2017. Quantifying the effectiveness of ecological restoration projects on long-term vegetation dynamics in the karst regions of Southwest China. Int. J. Appl. Earth Obs. Geoinf. 54, 105–113. https://doi.org/10.1016/j.jag.2016.09.013.

Tong, X., Brandt, M., Yue, Y., Horion, S., Wang, K., Keersmaecker, W. De, Tian, F., Schurgers, G., Xiao, X., Luo, Y., Chen, C., Myneni, R., Shi, Z., Chen, H., Fensholt, R., 2018. Increased vegetation growth and carbon stock in China karst via ecological engineering. Nat. Sustain. 1, 44–50. https://doi.org/10.1038/s41893-017-0004-x.

UNEP, 2011. Towards a Green Economy: Pathways to Sustainable Development and Poverty Eradication - A Synthesis for Policy Makers.

Wang, J.F., Hu, Y., 2012. Environmental health risk detection with GeogDetector. Environ. Model. Softw. 33, 114–115. https://doi.org/10.1016/j.envsoft.2012.01.015.

Wang, S.J., Liu, Q.M., Zhang, D.F., 2004. Karst rocky desertification in southwestern China: geomorphology, landuse, impact and rehabilitation. L. Degrad. Dev. 15, 115–121. https://doi.org/10.1002/ldr.592.

Wang, J., Wang, K., Zhang, M., Zhang, C., 2015. Impacts of climate change and human activities on vegetation cover in hilly southern China. Ecol. Eng. 81, 451–461. https://doi.org/10.1016/j.ecoleng.2015.04.022.

Wang, J.F., Zhang, T.L., Fu, B.J., 2016. A measure of spatial stratified heterogeneity. Ecol. Indic. 67, 250–256. https://doi.org/10.1016/j.ecolind.2016.02.052.

Wang, H., Gao, J., Hou, W., 2019a. Quantitative attribution analysis of soil erosion in different geomorphological types in karst areas: based on the geodetector method. J. Geogr. Sci. 29, 271–286. https://doi.org/10.1007/s11442-019-1596-z.

Wang, K., Zhang, C., Chen, H., Yue, Y., Zhang, W., Zhang, M., Qi, X., Fu, Z., 2019b. Karst landscapes of China: patterns, ecosystem processes and services. Landsc. Ecol. 34, 2743–2763. https://doi.org/10.1007/s10980-019-00912-w.

Wu, D., Zhao, X., Liang, S., Zhou, T., Huang, K., Tang, B., Zhao, W., 2015. Time-lag effects of global vegetation responses to climate change. Glob. Chang. Biol. 21, 3520–3531. https://doi.org/10.1111/gcb.12945.

Xu, E., Zhang, H., 2018. A spatial simulation model for karst rocky desertification combining top-down and bottom-up approaches. L. Degrad. Dev. 29, 3390–3404. https://doi.org/10.1002/ldr.3103.

Yan, X., Cai, Y.L., 2015. Multi-scale anthropogenic driving forces of karst rocky desertification in Southwest China. L. Degrad. Dev. 26, 193–200. https://doi.org/10.1002/ldr.2209.

Yang, J., Xu, X., Liu, M., Xu, C., Zhang, Y., Luo, W., Zhang, R., Li, X., Kiely, G., Wang, K., 2017. Effects of "Grain for Green" program on soil hydrologic functions in karst landscapes, southwestern China. Agric. Ecosyst. Environ. 247, 120–129. https://doi.org/10.1016/j.agee.2017.06.025.

Yang, Y., de Sherbinin, A., Liu, Y., 2020. China's poverty alleviation resettlement: progress, problems and solutions. Habitat Int 98, 102135. https://doi.org/10.1016/j.habitatint.2020.102135.

Yu, Y., Zhao, W., Martinez-Murillo, J., Pereira, P., 2020. Loess Plateau, from degradation to restoration. Sci. Total Environ. 738, 140206. https://doi.org/10.1016/j.scitotenv.2020.140206.

Zhang, J., Dai, M., Wang, L., Su, W., 2016a. Household livelihood change under the rocky desertification control project in karst areas, Southwest China. Land Use Policy 56, 8–15. https://doi.org/10.1016/j.landusepol.2016.04.009.

Zhang, J.Y., Dai, M.H., Wang, L.C., Zeng, C.F., Su, W.C., 2016b. The challenge and future of rocky desertification control in karst areas in southwest China. Solid Earth 7, 83–91. https://doi.org/10.5194/se-7-83-2016.

Zhang, C., Qi, X., Wang, K., Zhang, M., Yue, Y., 2017. The application of geospatial techniques in monitoring karst vegetation recovery in southwest China: a review. Prog. Phys. Geogr. 41, 450–477. https://doi.org/10.1177/0309133317714246.

Zhang, M., Wang, K., Liu, H., Zhang, C., Yue, Y., Qi, X., 2018. Effect of ecological engineering projects on ecosystem services in a karst region: a case study of northwest Guangxi, China. J. Clean. Prod. 183, 831–842. https://doi.org/10.1016/j.jclepro.2018.02.102.

Zhang, Z., Huang, X., Zhou, Y., 2020. Factors influencing the evolution of human-driven rocky desertification in karst areas. L. Degrad. Dev., ldr.3731 https://doi.org/10.1002/ldr.3731.

Zhao, S., Pereira, P., Wu, X., Zhou, J., Cao, J., Zhang, W., 2020. Global karst vegetation regime and its response to climate change and human activities. Ecol. Indic. 113, 106208. https://doi.org/10.1016/j.ecolind.2020.106208.

Zhao, R., Zhan, L., Yao, M., Yang, L., 2020. A geographically weighted regression model augmented by Geodetector analysis and principal component analysis for the spatial distribution of PM2.5. Sustain. Cities Soc. 56, 102106. https://doi.org/10.1016/j.scs.2020.102106.

Zhou, Y., Liu, Y., 2019. The geography of poverty: review and research prospects. J. Rural. Stud. https://doi.org/10.1016/j.jrurstud.2019.01.008.

Zhou, X., Lei, K., Khu, S.T., Meng, W., 2016. Spatial flow analysis of water pollution in eco-natural systems. Ecol. Indic. 69, 310–317. https://doi.org/10.1016/j.ecolind.2016.04.041.

Zhou, Q., Luo, Y., Zhou, X., Cai, M., Zhao, C., 2018. Response of vegetation to water balance conditions at different time scales across the karst area of southwestern China—a remote sensing approach. Sci. Total Environ. 645, 460–470. https://doi.org/10.1016/j.scitotenv.2018.07.148.

Zhou, L., Wang, X., Wang, Z., Zhang, X., Chen, C., Liu, H., 2020. The challenge of soil loss control and vegetation restoration in the karst area of southwestern China. Int. Soil Water Conserv. Res. 8, 26–34. https://doi.org/10.1016/j.iswcr.2019.12.001.

Zhu, Z., Piao, S., Myneni, R.B., Huang, M., Zeng, Z., Canadell, J.G., Ciais, P., Sitch, S., Friedlingstein, P., Arneth, A., Cao, C., Cheng, L., Kato, E., Koven, C., Li, Y., Lian, X., Liu, Y., Liu, R., Mao, J., Pan, Y., Peng, S., Peuelas, J., Poulter, B., Pugh, T.A.M., Stocker, B.D., Viovy, N., Wang, X., Wang, Y., Xiao, Z., Yang, H., Zaehle, S., Zeng, N., 2016. Greening of the Earth and its drivers. Nat. Clim. Chang. 6, 791–795. https://doi.org/10.1038/nclimate3004.